1st Latin-American Workshop on Structural Health Monitoring
LATAM-SHM 2023
December, 5-8 2023

ADVANCING WIND TURBINE SAFETY: VIBRATION-BASED EARLY DETECTION OF BLADE ICE ACCUMULATION USING EXTENDED ISOLATION FOREST

Abel Gómez[*], Christian Tutivén[*,†], Ricardo Prieto-Galarza[†,‡] and Yolanda Vidal[†,◇]

[*] Mechatronics Engineering
Faculty of Mechanical Engineering and Production Science, FIMCP
Escuela Superior Politécnica del Litoral, ESPOL
Campus Gustavo Galindo Km. 30.5 Vía Perimetral, P.O. Box 09-01-5863, Guayaquil, Ecuador
Phone number: +593 9 9103 5259,
e-mail: {afgomez, cjtutive}@espol.edu.ec,
web page: https://www.espol.edu.ec

[†]Control, Data, and Artificial Intelligence, CoDAlab
Department of Mathematics, Escola d'Enginyeria de Barcelona Est, EEBE
Universitat Politècnica de Catalunya, UPC
Campus Diagonal-Besós (CDB) 08019, Barcelona, Spain
e-mail: {ricardo.prieto, yolanda.vidal}@upc.edu,
Web page: https://www.upc.edu/es

[‡]Universidad Ecotec
Km. 13.5 Samborondón, Samborondón, EC092302 Ecuador

[◇]Institute of Mathematics (IMTech)
Universitat Politècnica de Catalunya (UPC)
Pau Gargallo 14, 08028 Barcelona, Spain
e-mail: yolanda.vidal@upc.edu - Web page: https://imtech.upc.edu/en

Key words: wind turbine, structural health monitoring, damage detection, blades, machine learning, extended isolation forest

Abstract. This study addresses the growing concerns around wind turbine safety and reliability, particularly focusing on the early detection of ice accumulation on blade surfaces, a critical factor affecting structural integrity and aerodynamic performance. It introduces an innovative methodology, combining vibration analysis with the advanced Extended Isolation Forest technique for effective detection of ice accumulation. This methodology uniquely utilizes normal operational data, which makes it widely applicable. It encompasses three stages: data collection and feature extraction from accelerometers, training the extended isolation forest algorithm on healthy turbine data, and subsequent evaluation through experiments with added masses. The results demonstrate its efficacy in early detection of ice accumulation, offering a proactive approach that reduces downtime, cuts repair costs, and mitigates ice-related risks. This methodology contributes to the advancement of structural health monitoring in wind turbines, improving operational safety and reliability, while providing operators with essential tools for risk mitigation, optimized maintenance, and long-term system performance.

1 INTRODUCTION

The rapid growth in wind turbine (WT) installations reflects a global shift toward renewable energy sources, driven by the need to reduce dependence on environmentally harmful fossil fuels. In 2018, the wind energy sector expanded significantly, with 51.3 GW of new capacity added, contributing to a total global capacity of 591 GW. Moreover, new onshore and offshore installations of over 55 GW each year are projected until 2023, according to GWEC [1]. Amidst this growth, attention is now focused on ensuring the long-term reliability and safety of WTs while simultaneously reducing operational costs. Maintenance expenses, especially for offshore installations subjected to extreme environmental conditions such as strong winds and waves, have emerged as a significant concern, accounting for up to 20% of total energy costs [2].

Structural health monitoring (SHM) emerges as a crucial tool in advancing wind energy. It enables real-time monitoring and predictive maintenance of WT critical components such as the tower, substructure (for offshore WTs), foundations, rotor, and blades. This study focuses on the detection of ice accumulation on WT blades, which is of paramount importance due to its significant impact on the structural integrity and aerodynamic performance of these devices. Ice build-up can trigger rotor imbalances, unwanted vibrations, and a reduction in power generation efficiency. Even when the ice accumulation is minimal, it has significant consequences on WT power production due to the degradation of aerodynamic performance associated with the deformation of the icy airfoil profile[3]. Moreover, it can pose safety risks and increase maintenance operational costs[4]. Hence, developing effective early detection methods for ice accumulation is essential to ensure the safe and efficient operation of WTs. For these reasons, the primary objective of this study is to develop an early detection method of ice accumulation on WT blades.

In the existing scientific literature, the issue of ice accumulation on WT blades has received attention, and various methods for detection have been explored. However, achieving early and precise detection of this phenomenon remains a challenge. Researchers have investigated approaches to address ice detection in WTs, yet there remains significant room for improvement in terms of the accuracy and effectiveness of these methodologies. In this study, vibration response accelerometer measurements are leveraged, and the extended isolation forest (EIF) is applied to develop an early detection approach for ice accumulation on WT blades. The primary advantage of this methodology lies in the exclusive use of healthy data for algorithm training and validation, enabling its applicability in various environments, as healthy data is prevalent in the industry. To validate the methodology, experimental testing on a laboratory WT blade is conducted to assess its effectiveness in detecting and diagnosing ice accumulation.

The results of the experiments demonstrate the methodology's effectiveness in detecting blade ice accumulation for a small amount of simulated ice mass. This finding holds significant implications for the wind energy sector, as it has the potential to greatly enhance turbine safety, operational performance, and reduce the economic impact of corrective maintenance.

The article follows a structured format as indicated in the following. Section 2 presents the experimental setup and the damage scenario. Section 3 indicates the methodology to be followed, covering topics such as data acquisition, feature extraction, and the EIF algorithm. Section 4 a summary of the experimental results obtained. Finally, Section 5 presents the conclusions.

2 Experimental setup

In the present study, a blade from a small WT (model E30PRO), with a length of 163 cm, is used. A vertical fixation is used, where the weight of the blade rests on its base, offering various options for securing it. Therefore, it is decided to place the blade vertically on a plate welded to a table measuring 850 × 850 × 150 mm. Eight triaxial acceleration sensors are installed at different positions on the blade. Each of these sensors records three signals (accelerations in the x, y, and z axes), resulting in a total of 24 acceleration measurements. To excite the structure (blade), an impact hammer is used to deliver 9 strokes in a period of 1 minute, simulating disturbances on the blade generated by the wind. Sensor placement is based on the Nielsen and Esu papers, respectively[5] [6], in which it is demonstrated that one of the best configurations for accelerometers involves placing 8 sensors distributed with 4 along the leading edge and 4 along the trailing edge, equidistantly. Additionally, it is considered that the sensors should be positioned in a way that maximizes the excitation of the measured property at that position, or at least obtains a sensitive sensor signal. Therefore, its placement is based on the hot spots present on the WT blade. In most cases, these spots are located between 30% and 70% of the length of the turbine [7] [8]. This sensor arrangement can be observed in Figure 1.

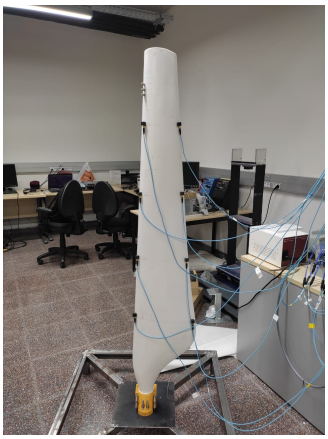

Figure 1: Experiment setup with sensors located on the leading and trailing edges along the blade.

Given that this work aims to detect the accumulation of ice masses on the WT blade (as it is a common type of damage), a configuration of bolts and nuts is used to mimic the masses resulting from ice formation. These are placed at the leading edge of the blade tip, as this is typically where ice mass formation begins [4]. For a better visualization of the location of these ice masses and the sensors, refer to the blade sketch shown in Figure 2.

In addition, Figure 3 shows the damage configuration (added mass) that is considered. This damage represents an ice mass formation of 35 g (3 bolts and 3 nuts per side). On the other hand, the healthy state of our structure is when no added mass is present.

3 Methodology

Next, the stages of the proposed methodology are listed. First, raw data from the sensors is collected. Second, data preprocessing is performed to ensure that each new sample contains sufficient and relevant data. Third, feature extraction is conducted for each experiment. Fi-

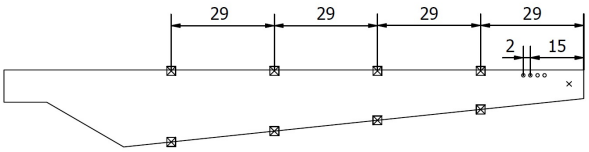

Figure 2: Contour of the blade where the squares indicate the location of the accelerometers vertically separated 29 cm with respect to the tip, the circles the position of the added masses (spaced 2 cm apart) and the cross the excitation zone with the hammer, the distances of the masses to the tip are referenced to the tip in centimeters.

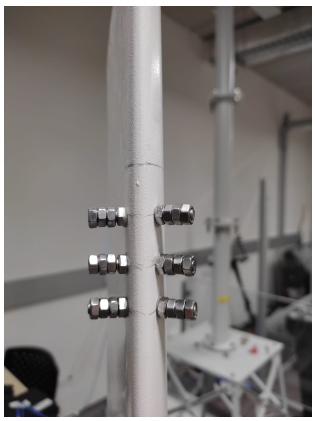

Figure 3: Representation of the damage case with added mass (simulated by bolts) of 35g.

nally, the architecture of an EIF algorithm designed to detect blade damage is described. The following subsections provide a comprehensive description of the various mentioned stages.

3.1 Data acquisition

The duration of each experimental trial for data acquisition is 60 seconds, with an approximate sampling frequency of 1706.67 Hz. Consequently, each of the 24 sensors (eight triaxial sensors) produces 102400 measurements. In these readings, a medium-force impact strike from an impact hammer is consistently applied at 6-second intervals, resulting in 9 significant strokes within 60 seconds. Below, is provided a description of the conducted trials:

- Two hundred and twenty healthy experimental trials without added mass (representing the healthy state).
- Twenty experimental trials with an added mass of 35 grams (representing the damage state).

Equation (1) shows the representation of the data obtained in each experimental trial in a general format (the same representation applies to all experiments, whether they are healthy or damaged cases). Where k represents each experimental trial, i.e. $k \in [1, K]$, where K is 240. The subscripts, in the matrix coefficients, represent readings over time (row) and sensor (column), respectively. More specifically.

- $n = 1, \ldots, N$ identifies the time instant, while N is the total number of time instants per experiment, equal to 102400;

- $m = 1, \ldots, M$ represents each sensor, while M is the total number of sensors, equal to 24.

$$X^{(k)} = \begin{bmatrix} x_{1,1}^{(k)} & x_{1,2}^{(k)} & \cdots & x_{1,M}^{(k)} \\ x_{2,1}^{(k)} & x_{2,2}^{(k)} & \cdots & x_{2,M}^{(k)} \\ \vdots & \vdots & \ddots & \vdots \\ x_{N,1}^{(k)} & x_{N,2}^{(k)} & \cdots & x_{N,M}^{(k)} \end{bmatrix}, \tag{1}$$

As a result, each experimental trial matrix $X_{N,M}^{(k)} \in \mathbb{M}_{102400\times 24}^{(k)}(\mathbb{R})$.

3.2 Data Reshape

In this section, a feature engineering technique, data reshaping, is applied to ensure that each of the samples processed by the algorithm contains useful and sufficient information from each sensor to determine the state of the structure.

In this study, samples that contain information from approximately two seconds of data are acquired, after each excitation from the stroke. Given that the sampling frequency is 1706.67 Hz, each sample contains 3414 values from each column. Therefore, the process to obtain these experiments is achieved through the following steps (the reshaping process is carried out for each experimental case):

1. Each column in the experimental test matrix is divided into 6-second time windows (10240 data points) because each impact occurs within that duration, and the initial 6 seconds are removed as they do not provide useful information;

2. From each sample, the first two seconds following the impact are selected (3414 data points), i.e., from the 6th to the 8th second, 12th to 14th second, and so forth, as illustrated in Figure 4. This is done to capture only the relevant information (impact), while the remaining values correspond to the time during which the disturbance caused by the impact stabilizes;

3. The data sequences are arranged as rows, with each new row added beneath the last one. In other words, there are 9 rows for each experimental trial;

4. These steps are repeated for all columns (sensors), generating new submatrices and appending them to the right of the last column corresponding to each sensor in the data matrix. The total number of horizontal submatrices is 24, one for each sensor.

As a result of this data reshaping process, a new matrix $Z^{(k)}$ is constructed as shown in Eq. (2).

$$Z^{(k)} = \left[\; Z^{(k),1} \;\middle|\; Z^{(k),2} \;\middle|\; Z^{(k),3} \;\middle|\; Z^{(k),4} \;\middle|\; \cdots \;\middle|\; Z^{(k),M} \;\right], \tag{2}$$

where each submatrix $Z^{(k),m}$ is represented by

$$Z^{(k),m} = \begin{bmatrix} z_{1,1}^{(k),m} & \cdots & z_{1,O}^{(k),m} \\ z_{2,1}^{(k),m} & \cdots & z_{2,O}^{(k),m} \\ \vdots & \ddots & \vdots \\ z_{J,1}^{(k),m} & \cdots & z_{J,O}^{(k),m} \end{bmatrix}, \tag{3}$$

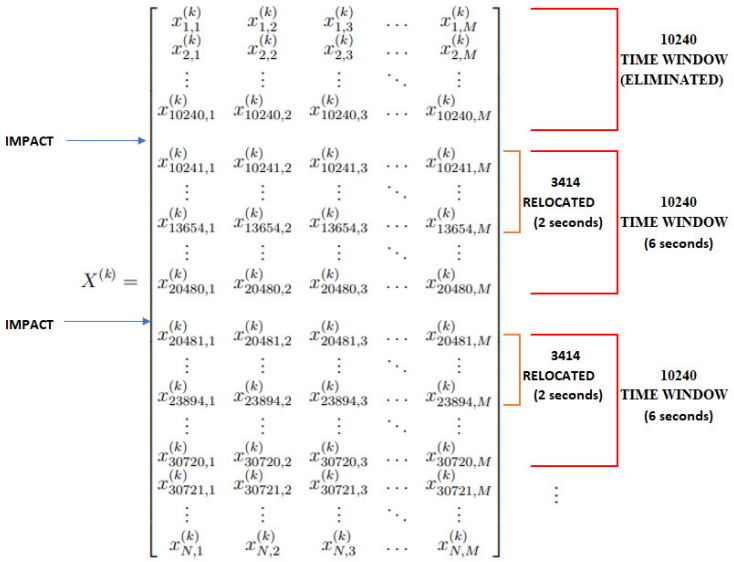

Figure 4: Data reshaping process.

where O represents the length of a time sequence, which is determined by taking the two seconds following the signal peak of the first sensor, i.e. O is equal to 3414, and $j = 1, \ldots, J$ identifies the sequence number, while J is the number of sequences per experiment, equal to 9. As a result, each $Z^{(k),m} \in \mathbb{M}_{9\times 3414}(\mathbb{R})$. This reshaping is performed for each experimental trial, whether it is a healthy or a damage case, as observed in the previous section.

3.3 Data Split

To ensure the proper training of the model, the experiments are divided into three sets: training, validation, and test, using the following percentages:

- Training Set: comprising 75% of the healthy data, this set contains 165 exclusively healthy experimental trials in total.
- Validation Set: consisting of 10 % of the healthy data, this set contains 22 exclusively healthy experimental trials in total.
- Test Set: This set includes 15 % of the remaining healthy data (33 experimental trials), and 100 % of the data with damage, i.e. 20 experimental trials with the damage case (added mass of 35 g).

These three data sets serve different purposes in evaluating model performance. The training set is used for the primary purpose of training the model, allowing it to become familiar with the data. In contrast, the validation set plays a crucial role in the unbiased evaluation of the model's training progress. It also allows to adjust the hyperparameters to avoid overfitting and to ensure the generalization of the model to unknown data. Finally, the test suite comes into play once the model has undergone full training. It serves as a final benchmark, as it evaluates the model's accuracy and performance on previously unseen data and provides a robust assessment of its predictive capabilities by focusing on the detection of damage cases.

3.4 Feature extraction

Feature engineering is a critical preprocessing step in data analysis, involving the creation of novel features derived from existing ones [9]. In the context of this study, new features are extracted.

To streamline and enhance the model training process in this study, three distinct features have been selected for each sensor: fractal dimension (FD), permutation entropy (PE), and kurtosis ($Kurt$). In the following subsection, two of these features are explained in detail, which are calculated on each of the matrices of Eq. (3). After the feature processing phase, considering that each sensor has these three features computed, it results in a modification of the data matrix dimensions, as exemplified in Table 1.

Table 1: New dimensionality of the matrix, after feature extraction.

Structural State	Set	Matriz Dimensionality
Healthy	Training	1485 x 72
Healthy	Validation	198 x 72
Healthy	Test	297 x 72
Damage	Test	180 x 72

3.4.1 Fractal Dimension

Fractal Dimension (FD) is a metric used to evaluate the complexity and irregularity of geometric structures or datasets[10]. In this research, FD is applied to analyze acceleration signals from WT blade sensors, with the aim of identifying irregular patterns as potential indicators of blade issues and providing additional insights beyond mean and standard deviation statistics. The Katz method is used for the FD calculation, which involves comparing the curve length with the straight-line distance. The formula for FD in this study is as follows:

$$FD(z_{j,\cdot}^{(k),m}) = \frac{\log(L(z_{j,\cdot}^{(k),m}))}{\log(d(z_{j,\cdot}^{(k),m}))} \tag{4}$$

where

- FD($z_{j,\cdot}^{(k),m}$) denotes the Katz's FD for the j^{th} row of $Z^{(k),m}$ matrix.
- $L(z_{j,\cdot}^{(k),m})$ represents the length of the curve for the j^{th} row, calculated as the cumulative sum of the Euclidean distances between successive points in the signal.
- $d(z_{j,\cdot}^{(k),m})$ is the maximum distance from any point in the signal to the initial point, essentially indicating the largest difference between the signal values in the j^{th} row of the $Z^{(k),m}$ matrix and the initial signal value.

Katz introduced a normalization technique for 'd' and 'L' using the average step length, denoted as 'a,' which is calculated as

$$a = \frac{L}{N}, \tag{5}$$

where 'N' is the total number of steps of the curve, which in our context is represented by the variable 'O'. This leads to the modified formula:

$$FD(z_{j,\cdot}^{(k),m}) = \frac{\log(\frac{L(z_{j,\cdot}^{(k),m})}{a})}{\log(\frac{d(z_{j,\cdot}^{(k),m})}{a})} = \frac{\log(O)}{\log(\frac{d(z_{j,\cdot}^{(k),m})}{L(z_{j,\cdot}^{(k),m})}) + \log(O)} \tag{6}$$

3.4.2 Permutation Entropy

PE is a widely used metric in time series and signal analysis to assess data complexity and regularity, known for its conceptual simplicity and computational efficiency[11]. In this section, we provide an in-depth exploration of PE and its application within the scope of this study. PE is based on permutations, where data sequences are rearranged to assess regularity by quantifying the transformations needed to change from an ordered to a disordered sequence, shedding light on data regularity and randomness[12]. The underlying formula for PE involves permutation calculations applied to specific data sequences and can be expressed as follows.

$$\mathrm{PE}(z_{j,\cdot}^{(k),m}) = -\sum_{l=1}^{n!} p(\pi_l)\log(p(\pi_l)), \tag{7}$$

where:

- $\mathrm{PE}(z_{j,\cdot}^{(k),m})$ represents the PE of the j^{th} row of $Z^{(k),m}$ matrix.
- $n!$ is the factorial of n, indicating the total number of possible ordinal patterns or permutations of length n.
- $p(\pi_l)$ is the probability of occurrence of the l^{th} permutation π_l in the time series.

In the context of this study, the PE is applied to the acceleration signals recorded by sensors on the WT blades, for which use is made of an entropy dimension of $n = 6$ and an embedding delay $\tau = 14$ guided by the study of Audun Myers, et al. [12]. This metric is used to characterize the structure and patterns of vibrations in the blades, playing a crucial role in the early detection of anomalies or damage.

3.5 Normalization

Data normalization, a crucial aspect of data analysis and machine learning, aims to standardize feature scales for equal contributions in analysis and modeling, preventing dominance by features with larger scales[13]. In our study on early ice accumulation detection on WT blades, data normalization is particularly vital due to feature magnitude variations. We selected the Z-Score method to normalize data obtained from feature extraction, transforming all 72 columns in the training dataset to have a mean of zero and a standard deviation of one. Using these statistics, we normalized columns in validation and test datasets (both healthy and damaged) to ensure uniform scaling, making the data EIF algorithm-ready.

3.6 Extended Isolation Forest

Unlike many anomaly detection methods that focus on modeling normal behavior, EIF, an extension of the Isolation Forest (IF), is designed to explicitly identify anomalies. It leverages two key characteristics of anomalies: their rarity and significantly different attribute values[14]. IF constructs binary trees using random subsamples from the dataset, with parameters for subsampling and the number of trees controlling model complexity[15]. Each tree splits the data based on randomly selected attributes until reaching nodes containing one instance or those with identical values. The anomaly score is determined by the path length through the tree and takes values in the (0, 1) range, with scores close to 1 indicating anomalies. To address biases in branching approaches, EIF introduces hyperplane selection to generate more consistent anomaly scores. The extension level can be adjusted based on the number of feature axes, which in this study ranges from 0 to 71, allowing for precise adaptation to the 72 available features. This range was chosen considering that a "fully extended" level would encompass all features but without redundancy, ensuring a tailored model fitting the data's feature count.

4 Results

In this section, the results of the failure prediction methodology based on the EIF model described in the previous section are presented and discussed.

First, the hyperparameters for the EIF algorithm's architecture are determined using the training and validation datasets. To streamline this process, the Python framework Optuna is utilized for automated hyperparameter tuning. The hyperparameters outlined in Table 2 are obtained.

Table 2: Hyperparameters of the EIF algorithm.

Number of Trees	Size of subsample	Extension Level
434	41	3

The data are organized into groups of 27 consecutive time segments (three experiments of 60 seconds each). This approach provided a concise and visual summary of the data distribution, facilitating the identification of damages. As can be seen in 5 (left) the maximum median of the anomaly score boxplots from all training experiments is equal to 0.493. This value is defined as the fault detection threshold for the validation and testing data set. Since the model is trained exclusively on data considered as "healthy", this threshold becomes a key reference. Any data falling below this threshold is classified as "healthy", while those above it are considered "anomalous" or indicative of damage. On the other hand, as can be seen in Figure 5 (right), none of the boxplots of the validation experiments exceed the predefined threshold, showing that the model generalizes well with the selected EIF hyperparameters.

To evaluate the performance test data corresponding to damage conditions are analyzed. In Figure 6 (left), it can be seen that the damage state group of sequences is classified as anomaly, showing the efficiency of the model in detecting damage. On the other hand, Figure 6 (right) depicts the analysis of test data related to the healthy state. In this case, it is observed that no group of segments is classified as an anomaly, which is correct.

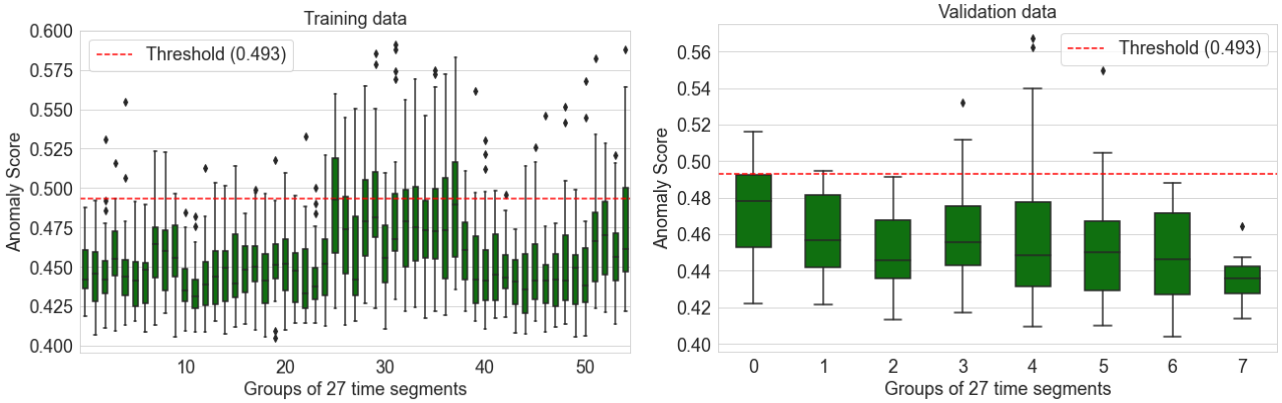

Figure 5: Boxplot of the anomaly scores corresponding to the grouping of 27 test data time segments. Training data on the left, and validation data on the right.

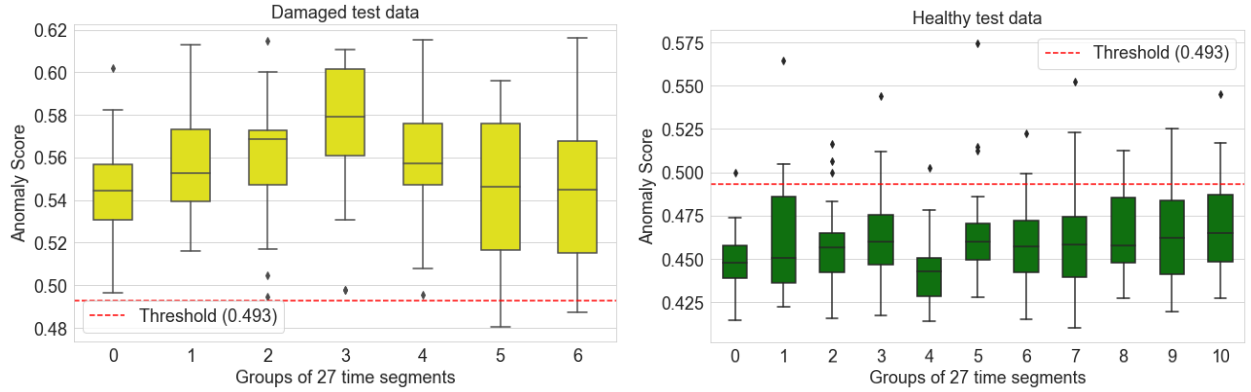

Figure 6: Boxplot of the anomaly scores corresponding to the grouping of 27 test data time segments. Damage data on the left, and healthy data on the right.

Consequently, it is concluded that to improve the results, the option is made to use the median of grouping 27 consecutive time segments as the metric for anomaly detection, resulting in a precision rate 100% when detecting structural damage with the EIF algorithm.

5 Conclusions

This study developed a methodology for the early detection of ice accumulation on WT blades, a critical issue affecting their structural integrity and performance. The methodology, based on the vibration response and the EIF, is proven to be effective in detecting and diagnosing ice accumulation, even in small quantities like 35 grams. This ability allows for prompt decision making, reducing inspection downtime, maintenance costs, and unexpected breakdowns. In particular, the methodology relies solely on healthy data for training and validation, making it applicable in various industrial settings. In conclusion, this research offers a valuable tool for improving safety and efficiency in the wind energy industry, potentially reducing operational costs.

ACKNOWLEDGMENTS

This work is partially funded by the Spanish Agencia Estatal de Investigación (AEI) - Ministerio de Economía, Industria y Competitividad (MINECO), and the Fondo Europeo de Desarrollo Regional (FEDER) through the research projects PID2021-122132OB-C21 and TED2021-129512B-I00; and by the Generalitat de Catalunya through the research project 2021-SGR-01044.

REFERENCES

[1] G. W. E. Council, Gwec global wind report 2019, Global Wind Energy Council: Bonn, Germany (2017).

[2] M. Mieloszyk, W. Ostachowicz, An application of structural health monitoring system based on fbg sensors to offshore wind turbine support structure model, Marine Structures 51 (2017) 65–86.

[3] F. Martini, L. T. Contreras Montoya, A. Ilinca, Review of wind turbine icing modelling approaches, Energies 14 (16) (2021) 5207.

[4] M. Virk, F. Afzal, Review of icing effects on wind turbine in cold regions (2018).

[5] J. S. Nielsen, D. Tcherniak, M. D. Ulriksen, Quantifying the value of shm for wind turbine blades, in: 9th European Workshop on Structural Health Monitoring, NDT net, 2018, p. 168.

[6] O. O. Esu, J. A. Flint, S. J. Watson, Integration of low-cost accelerometers for condition monitoring of wind turbine blades, system 14 (2013) 15.

[7] C. C. Ciang, J.-R. Lee, H.-J. Bang, Structural health monitoring for a wind turbine system: a review of damage detection methods, Measurement science and technology 19 (12) (2008) 122001.

[8] P. Rizk, N. Al Saleh, R. Younes, A. Ilinca, J. Khoder, Hyperspectral imaging applied for the detection of wind turbine blade damage and icing, Remote Sensing Applications: Society and Environment 18 (2020) 100291.

[9] A. Zheng, A. Casari, Feature engineering for machine learning: principles and techniques for data scientists, " O'Reilly Media, Inc.", 2018.

[10] E. Hoxha, Y. Vidal, F. Pozo, Damage diagnosis for offshore wind turbine foundations based on the fractal dimension, Applied Sciences 10 (19) (2020) 6972.

[11] M. Henry, G. Judge, Permutation entropy and information recovery in nonlinear dynamic economic time series, Econometrics 7 (1) (2019) 10.

[12] A. Myers, F. A. Khasawneh, On the automatic parameter selection for permutation entropy, Chaos: An Interdisciplinary Journal of Nonlinear Science 30 (3) (2020).

[13] D. Singh, B. Singh, Investigating the impact of data normalization on classification performance, Applied Soft Computing 97 (2020) 105524.

[14] L. Sun, S. Versteeg, S. Boztas, A. Rao, Detecting anomalous user behavior using an extended isolation forest algorithm: an enterprise case study, arXiv preprint arXiv:1609.06676 (2016).

[15] R. B. de Santis, M. A. Costa, Extended isolation forests for fault detection in small hydroelectric plants, Sustainability 12 (16) (2020) 6421.